Journal of Physics: Conference Series

PAPER • **OPEN ACCESS**

Absolute efficiency calibration of a coaxial HPGe detector for quantitative PGAA and T-PGAA

To cite this article: A Parmentier *et al* 2018 *J. Phys.: Conf. Ser.* **1055** 012010

View the article online for updates and enhancements.

Related content

- Efficiency calibrations of HPGe detector for PGNAA system
  S Sangaroon, W Ratanatongchai, C Wichaisri et al.
- Operation of an 18-fold segmented n-type HPGe detector in liquid nitrogen
  I Abt, A Caldwell, D Gutknecht et al.
- Production of the 178m2Hf isomer using a 1.2 GeV electron accelerator
  V I Kirischuk, A M Dovbnya, S S Kandybei et al.

IOP ebooks™

Bringing you innovative digital publishing with leading voices to create your essential collection of books in STEM research.

Start exploring the collection - download the first chapter of every title for free.

This content was downloaded from IP address 5.170.124.225 on 05/08/2018 at 12:08

IOP Conf. Series: Journal of Physics: Conf. Series **1055** (2018) 012010 doi:10.1088/1742-6596/1055/1/012010

Absolute efficiency calibration of a coaxial HPGe detector for quantitative PGAA and T-PGAA

A Parmentier[1], L Arcidiacono[1,2,4], R Senesi[1,3,4,*], G Romanelli[5], C Andreani[1,3,4], J Moir[5], and G Festa[4]

[1] NAST Center and Dipartimento di Fisica, Università degli Studi di Roma "Tor Vergata", via della Ricerca Scientifica 1, 00133 Rome, Italy
[2] UCL-Institute of Archaelogy, University College London, 31-34 Gordon Square, London WC1H 0PY, UK
[3] CNR-IPCF Sezione di Messina, viale Ferdinando Stagno d'Alcontres 37, 98158 Messina, Italy
[4] Centro Fermi-Museo Storico della Fisica and Centro Studi e Ricerche "Enrico Fermi", piazza del Viminale 1, 00184 Rome, Italy
[5] ISIS Facility, Rutherford Appleton Laboratory, Chilton, Didcot, Oxfordshire, OX11 0QX, UK

E-mail: roberto.senesi@uniroma2.it

Abstract. Following international guidelines by the IEEE and a well-established calibration procedure developed at the Hungarian Institute of Isotopes in Budapest, the experimental absolute efficiency calibration of an Ortec n-type coaxial high-purity germanium (HPGe) detector (GMX Profile series) has been performed, in view of direct application to quantitative PGAA and T-PGAA investigations of Cultural Heritage multicomponent manufacts.

1. Introduction

Among the several characteristics of a γ-ray detector, the absolute full-energy-peak (FEP) efficiency (*i.e.*, the ratio of the number of counts under the photopeak to the total number of γ-rays emitted by the source) plays a vital role for quantitative spectroscopy, especially when complex γ-ray spectra involving many lines are under scrutiny. In particular, the development of Prompt-Gamma Activation Analysis (PGAA) and Time-resolved Prompt-Gamma Activation Analysis (T-PGAA) capabilities at pulsed neutron sources has allowed to expand the potential of PGAA at continuous sources for the study of functional materials and Cultural-Heritage samples [1–3]. These investigations require the use of high-resolution γ-ray detectors to resolve the complex spectra of multicomponent samples.

In this field, semiconductor detectors are much appreciated in comparison to inorganic scintillators such as NaI(Tl), due to their superior energy resolution when operated at low temperatures. However, this improved energy resolution comes along with a major drawback, since the generally smaller sizes of common germanium detectors, together with the lower atomic number of Ge with respect to iodine, lowers the FEP efficiency (ϵ_{fep}) by an order of magnitude in typical cases [4].

For this reason, the assessment of the absolute $\epsilon_{fep}(E)$ curve (*i.e.*, ϵ_{fep} as a function of photon energy) of a HPGe detector becomes a crucial analytic passage, also taking into account the unknown exact functional dependence of efficiency on energy (only partially fixed by the

Content from this work may be used under the terms of the Creative Commons Attribution 3.0 licence. Any further distribution of this work must maintain attribution to the author(s) and the title of the work, journal citation and DOI.
Published under licence by IOP Publishing Ltd

Table 1: Source features, from source datasheet and LNE-LNHB/CEA nuclear-data tables [9]. The most important acquisition parameters are reported as well: A_0 = reference activity (3% uncertainty with 95% confidence), $t_{\frac{1}{2}}$ = half time, t_{live} = livetime, *i.e.*, total time of actual count acquisition with no dead time included, and d = source-detector distance.

			Set 1		Set 2	
	A_0	$t_{\frac{1}{2}}$	t_{live}	d	t_{live}	d
^{60}Co	(42.10 ± 1.26) kBq	5.2711 ± 0.0008 y	7200 s	11.5 cm	300 s	11.5 cm
^{133}Ba	(36.60 ± 1.10) kBq	10.539 ± 0.006 y	7200 s	11.5 cm	300 s	11.5 cm
^{137}Cs	(41.10 ± 1.23) kBq	30.05 ± 0.08 y	7200 s	11.5 cm - 1 cm	300 s	11.5 cm 3.7 cm 0.5 cm
^{241}Am	(39.60 ± 1.19) kBq	432.6 ± 0.6	7200 s	11.5 cm	300 s	11.5 cm

application of empirical or semi-empirical models [5]), as well as limits to the overall accuracy due to unavoidable sources of uncertainty hidden in the geometry of the experimental setup.

The 1996 IEEE protocol, which establishes terminology and standard test procedures for germanium γ-ray detectors [6], contains popular guidelines to perform various types of calibrations. Its integration to the novel efficiency-calibration procedure developed at the Hungarian Institute of Isotopes in Budapest [5, 7] allows for the improvement of some practices, such as the assessment of the system non-linearity, which is mainly due to the analog-to-digital converter (ADC), and is cause to major FEP distorsions that cannot be neglected when (T-)PGAA is performed because of the very low amplifier gains employed in this technique [8]. Starting from a careful mix of such protocols, the experimenter is allowed to perform the ϵ_{fep} calibration of a HPGe detector over a wide energy range ($\sim$ 0.05-11.00 MeV), typically making use of a large set of calibrated and noncalibrated samples of radionuclides over the low-energy region (up to about 2 MeV), while exploiting cascades from thermal-neutron capture on non-calibrated, non-commercial light-nucleus targets (such as ^{14}N or ^{35}Cl) over the high-energy counterpart (above 2 MeV) [5].

In the present work, a practical application of this procedure is presented for the assessment, over the low-energy region, of the absolute $\epsilon_{fep}(E)$ curve of an Ortec n-type coaxial HPGe detector (GMX Profile series).

2. Experimental setup

The thermostated HPGe detector shown in Fig. 1 was employed to collect a double set of γ spectra of an ensemble of 4 calibrated radionuclides (reference time: t_0 = 01/11/2005) in a shielded area located in the Target Station 2 (TS2) building at the ISIS pulsed neutron and muon source [10], UK. Measurements included "beam-off" background (both measurement sets were collected in the course of a mainteinance shutdown of all ISIS beamlines, in order to minimize unwanted signals in the spectra).

A summary of source features and major acquisition parameters is reported in Table 1. In step with the IEEE protocol [6], discoidal standards were used with an active nucleus of $\leq$ 2 mm in diameter, and the livetime of the background collection was consistent with the one of any source spectrum. Distances from the crystal - which do not include the gap (2.6 cm) between the endcap and crystal - were shortened in comparison to the customary 25-cm value, due to the very low activities of the sources. These distances were chosen as a reasonable trade-off

Figure 1: The Ortec coaxial HPGe detector used for measurements.

between maximization of signal-to-noise (S/N) ratio and minimization of coincidence summing (which induces FEP loss). Additional distances for ^{137}Cs were taken for future employment in simulations.

Following the same route, a second batch of measurements (Set 2) was taken in order to correct source placement (according to a coaxial geometry, Fig. 2) and fix the non-optimal polarization of the semiconductor junction by switching to -3800 V in the high-voltage (HV), compared to the initial -1800 V value.

No collimation and/or Compton-suppression arrangement were used.

3. Data reduction and analysis

After a channel-by-channel background subtraction from any source spectrum, corresponding spectra in Sets 1 and 2 were compared to one another. Though the former show larger S/N ratios (a neat example is shown in Fig. 3 for barium), the latter were chosen for subsequent analysis due to the significant reduction in the left skewing of peaks following HV correction (an example is presented in Fig. 4 for cobalt), with consequent enhancement of spectral resolution, lowering of the low-energy threshold down to about 20 keV, and removal of any possible multi-peak fitting of single lines.

The first part of the data analysis was performed by Hypermet-PC software [8, 11], which is currently considered the most reliable - though closed-source - package for the automated analysis of complex γ-ray spectra [12]. The procedure outlined below follows the indications reported in [5]. After direct editing and update of the Hypermet-PC database of nuclear data (originally dating back to the early 2000s), the following relationship

$$E = a + m \cdot Ch, \tag{1}$$

where a (in keV, like E) and m represent the intercept and slope, respectively, of the calibration line, while Ch is the position of the peak centroid (in channels), was used to perform an initial energy pair-calibration (*i.e.*, the conversion of channels into energies) for each spectrum with no consideration - at a first approximation - of non-linearity effects introduced by the ADC.

This calibration was used to perform a first fit of each spectrum ("peaklist 0"), taking into account that the i^{th} peak profile in the j^{th} channel is formalized as:

Figure 2: Source placement for Set 2.

$$p(j) = \Gamma_i e^{-\left(\frac{j-j_{i,0}}{\delta}\right)^2} + \frac{1}{2} A_i e^{\frac{j-j_{i,0}}{\beta}} erfc\left(\frac{\delta}{2\beta} + \frac{j-j_{i,0}}{\delta}\right), \tag{2}$$

where the first term in the right part of the equation is a Gaussian of amplitude Γ_i and variance $\frac{\delta}{\sqrt{2}}$, and the second one is an exponentially-modified Gaussian (EMG) - of amplitude A_i, variance $\frac{\delta}{\sqrt{2}}$, and exponential-decay time constant β - representing the left skewing.

An additional baseline correction of the form:

$$S_i\, erfc\left(\frac{j-j_{i,0}}{\delta}\right) + \frac{1}{2} W_i e^{\frac{j-j_{i,0}}{\tau}} erfc\left(\frac{\delta}{2\tau} + \frac{j-j_{i,0}}{\delta}\right) + c_0 + c_1 j + c_2 j^2, \tag{3}$$

was applied, including in progressive order:

- an error function of amplitude S_i, which accounts for photons scattered at small angles;
- a "tail"contribution (EMG with exponential-decay time constant $\tau \gg \beta$), which accounts for detector surface-effects, especially at very low energies;
- a parabolic contribution with polynomial coefficients c_0, c_1, and c_2.

A higher-order refinement of the above fit ("peaklist 1") was, then, performed by a non-linearity assessment accomplished by construction of a non-linearity curve via orthonormal-polynomial least-square (OPLS) fit of source peak-positions in peaklist 0. This procedure - which consists of measuring the positions of the FEP centroids in the spectrum of a multi-emitter, and then evaluating their displacement from a calibration linear curve [5, 8] - is more accurate than the one suggested by the IEEE, which implies the use of a high-precision pulse generator at the test-input terminal of the pre-amplifier to "simulate" the electronic-noise contribution to the FEP FWHM [6].

Being only one multi-emitter (^{133}Ba) available in the calibration set, this initially limited result accuracy over the energy range $\geq$ 400 keV. The problem was bypassed via an *ad hoc* correction of centroid errors for ^{137}Cs and ^{60}Co by picking appropriate values reported in LNE-LNHB/CEA tables.

The ensemble of all peaklists 1 was finally used to perform the assessment of the intrinsic part of $\epsilon_{fep}(E)$, namely $\epsilon_{int}(E)$, that can be defined as [5]:

$$\epsilon_{int} = \frac{C}{P_\gamma N \frac{t_{live}}{t_{acq}}} \qquad \textit{(abs calibrated source)} \tag{4}$$

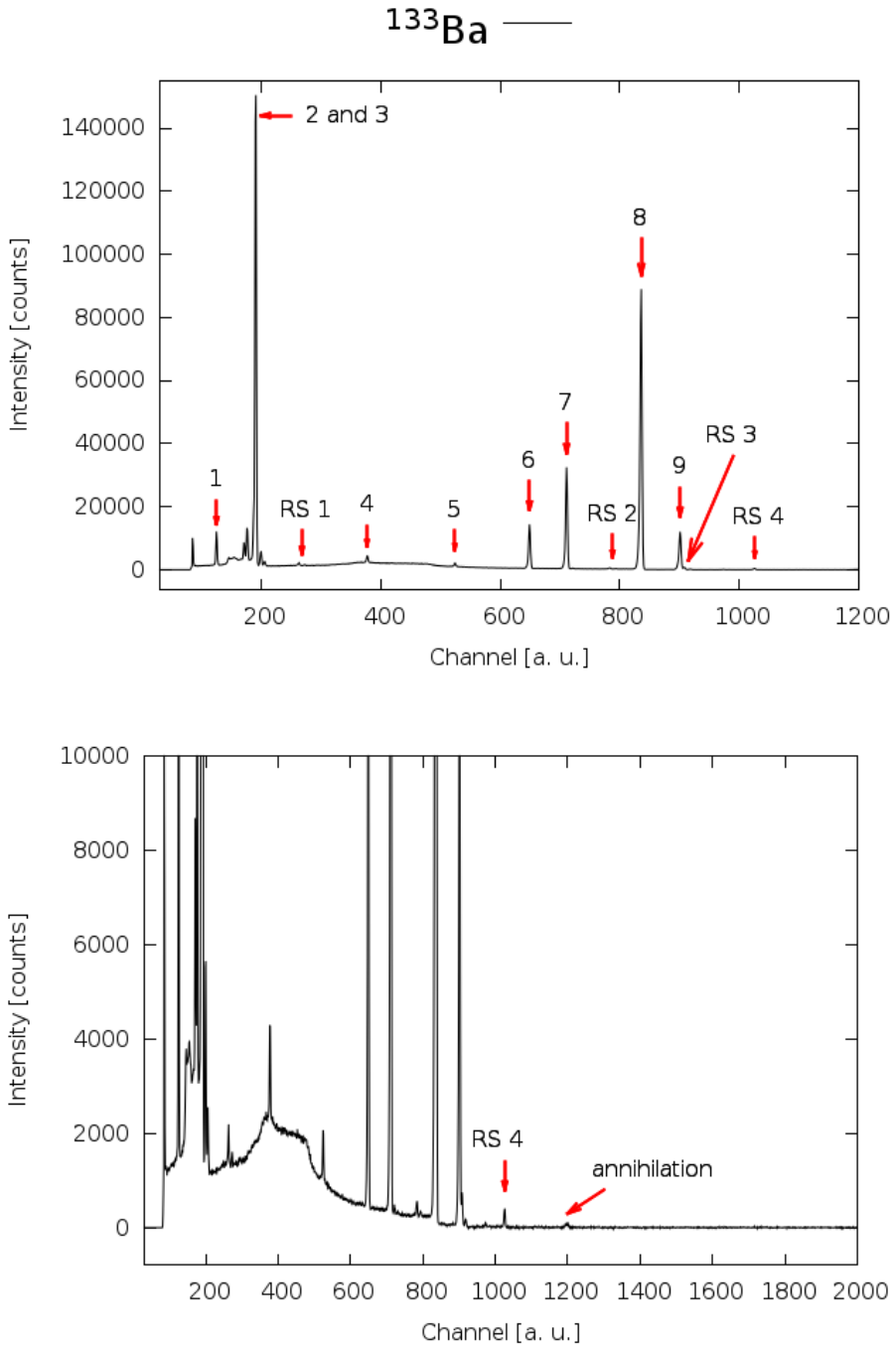

Figure 3: Top: ^{133}Ba γ spectrum (Set 1) up to energies of the order of 0.5 MeV. Gamma emissions from LNE-LNHB/CEA tables: 1 = 53.1622(18) keV, 2 = 79.6142(19) keV, 3 = 80.9979(11) keV, 4 = 160.6121(16) keV, 5 = 223.237(2) keV, 6 = 276.3992(21) keV, 7 = 302.8512(16) keV, 8 = 356.0134(17) keV, and 9 = 383.8491(12) keV. Visible random sums: RS 1 = peak 3 + $K_{\alpha,\beta}$ X lines of Cs, RS 2 = peak 7 + $K_{\alpha,\beta}$ X lines of Cs, RS 3 = peak 8 + $K_{\alpha,\beta}$ X lines of Cs, and RS 4 = peaks 2-3 + peak 8. Bottom: same spectrum (zoom) up to energies of 1 MeV, with a tentative assignment of the annihilation peak at 510.999 keV.

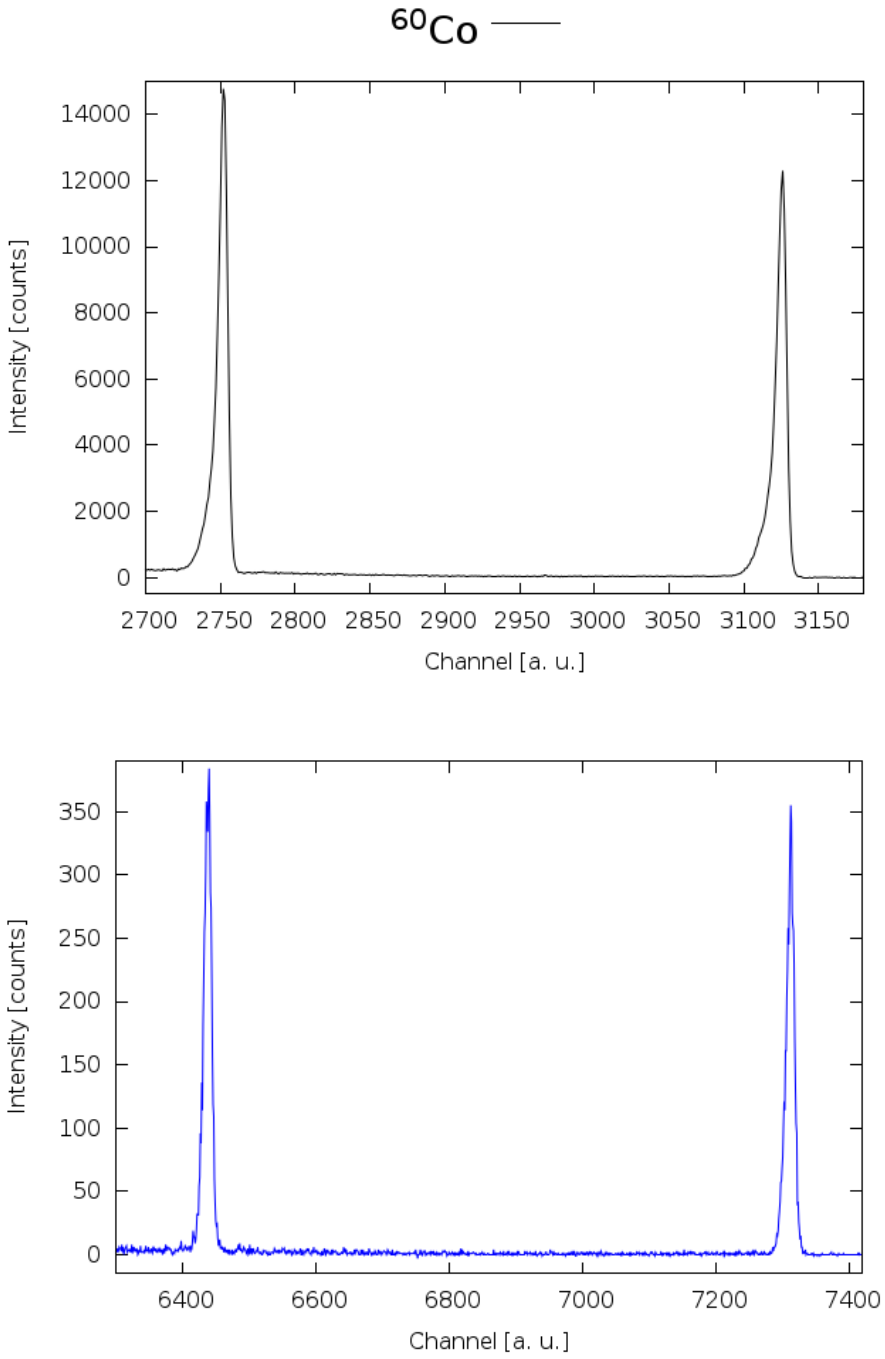

Figure 4: Top: 1.173- e 1.332-MeV lines of ^{60}Co in the Set-1 spectrum. Bottom: same lines in the correspondent Set-2 spectrum.

Table 2: Coefficients recovered by OPLS fitting (ROOT software) of discrete efficiency points associated with radionuclide peaks.

	a_0	a_1	a_2	a_3
grade 2	-1.979 ± 0.216	4.128 ± 0.082	-0.378 ± 0.007	-
grade 3	-29.776 ± 0.046	19.347 ± 0.014	-3.074 ± 0.002	0.1556 ± 0.0002

$$\epsilon_{int} = \frac{C}{P_\gamma} \qquad \textit{(non calibrated source)}, \tag{5}$$

where

- C = number of counts for each peak
- P_γ = γ-emission probability
- $N(t) = \frac{A_0}{\lambda} e^{-\lambda(t-t_0)}(1 - e^{-\lambda t_{acq}})$ = number of decays from the start of measurement
- t_{live} = livetime
- t_{acq} = acquisition time.

In this way, discrete efficiencies were calculated for each line of each radionuclide, selecting one source (^{133}Ba) as absolutely calibrated, and using it as a normalizing factor for the remaining standards (which practically corresponds, in the log-log scale, to an efficiency shift of ^{60}Co, ^{137}Cs, and ^{241}Am along the vertical axis to match ^{133}Ba values).

Then, an OPLS fit of the above discrete efficiency points, based on the commonly-used function [13, 14]

$$ln\left[\epsilon_{int}(E)\right] = \sum_{i=0}^{n} a_i [ln(E)]^i, \tag{6}$$

(linearized χ^2 method) was performed in order to get the desired $\epsilon_{int}(E)$ curve. Due to Hypermet-PC being proprietary software, the obtained curve could not be exported to a regular ASCII file. An external reconstruction of $\epsilon_{int}(E)$ was attempted, starting from fit coefficients a_i calculated by Hypermet-PC. Yet, even taking into account the remapping of energies onto the $(-1, 1)$ range operated by the software in order to improve the stability of the fitting algorithm [5, 15], no adequate correspondence was found, probably due to an unknown compression/expansion factor applied by Hypermet-PC to the curve. Consequently, a parallel fit (again by Eq. 6) of the same discrete efficiency points was performed via ROOT software [16], recovering the results summarized in Table 2 and Fig. 5. Low-grade polynomial functions were used in order to avoid any possible artificial oscillation of the resulting efficiency response curve in those regions covered by sporadic experimental points.

Finally, in Fig. 6 the grade-3 fit for $\epsilon_{int}(E)$ is shown together with its uncertainty region, after normalization to the mean value of the discrete intrinsic efficiency of the barium line at 160.6121 keV.

In order to get the global absolute FEP efficiency $\epsilon_{fep}(E) = \epsilon_{geom}\epsilon_{int}(E)$ for a point-source geometry, a multiplication must be performed by a geometric factor $\epsilon_{geom} = \frac{\Omega}{4\pi}$, with $\Omega = 2\pi\left(1 - \frac{d}{\sqrt{d^2+r^2}}\right)$ = solid angle "seen" by the detector, d = source distance from the crystal, and r = crystal radius. In our case, at $d = (11.5 + 2.6)$ cm and $r = 2.98$ cm, it is $\epsilon_{geom} = 0.011$, which explains the initial need for reducing the source-detector distance from 25 to 14.1 cm.

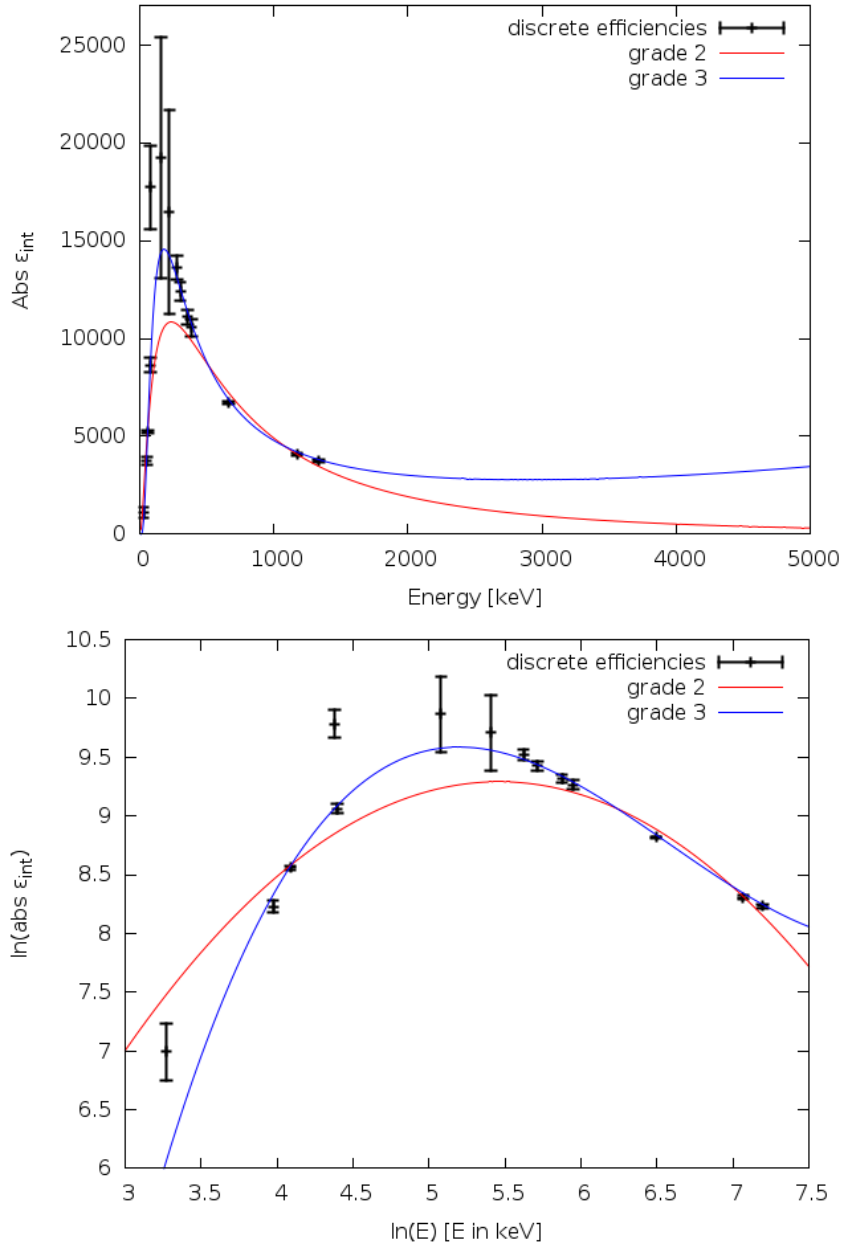

Figure 5: Top: lin-lin representation of the absolute intrinsic efficiency curves (grade 2 and 3) obtained by OPLS fitting (ROOT software) of discrete efficiency points associated with radionuclide peaks. Bottom: same curves in a log-log representation.

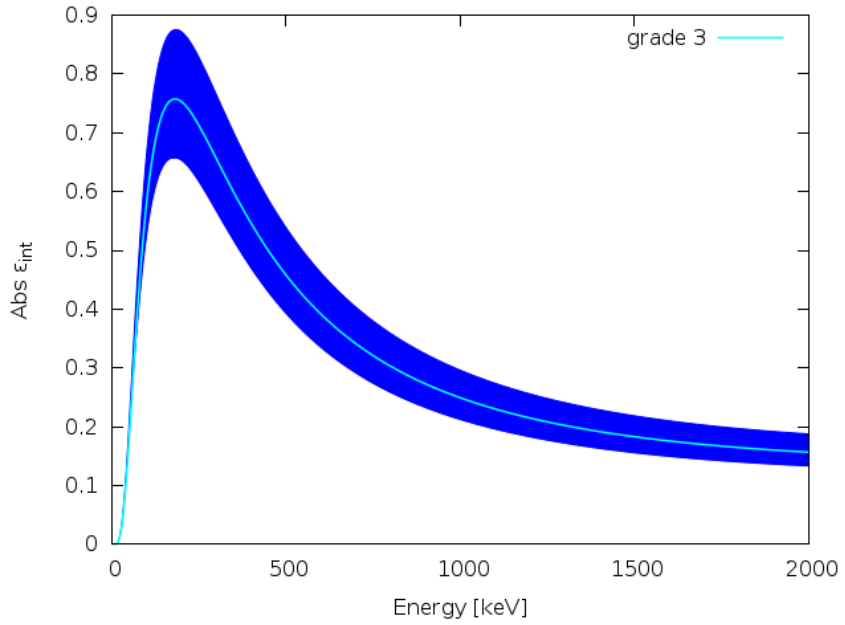

Figure 6: Lin-lin representation of the grade-3 fit for the absolute intrinsic efficiency $\epsilon_{int}(E)$, after normalization to the mean value of the discrete efficiency of barium line at 160.6121 keV - together with its uncertainty region.

4. Discussion

A quick look at Table 2 and Fig. 5 suggests that, in spite of the grade-3 fit showing an unphysical growth of the intrinsic efficiency curve in the high-energy region (where absorption cross-sections tend to decrease [7]), this same curve fits best the low-energy portion of the spectrum.

Consequently, we have opted for saving this grade-3 low-energy "patch", with the purpose to link it - by an appropriate continuity condition imposed on $\epsilon_{int}(E)$ at the matching point - to a high-energy complement obtained by future measurements on other non-calibrated sources, and/or ongoing Monte Carlo simulations of the detector efficiency, and/or similar data from the scientific literature.

5. Conclusions

The absolute efficiency of an Ortec n-type coaxial HPGe detector, used for PGAA and T-PGAA measurements on functional and Cultural Heritage samples at the ISIS pulsed neutron and muon source [2, 3, 17, 18], was determined by the exploitation of a set of calibrated γ-emitting sources following the procedures outlined in Refs. [5, 6]. The results are in agreement with the values reported in the literature [5, 19, 20].

This work will allow to carry out quantitative T-PGAA measurements on multicomponent samples, primarily addressing functional materials and Cultural Heritage artifacts, as well as quantitative estimates of the absolute γ background at ISIS beamlines.

Acknowledgements

This work was supported within the CNR-STFC Agreement 20142020 (No. 3420 20142020) concerning collaboration in scientific research at ISIS Spallation Neutron Source, and partially supported within the SMART Campus Project (Regione Lazio 2015-2017).

References

[1] Toh Y, Ebihara M, Kimura A, Nakamura S, Harada H, Hara K Y, Koizumi M, Kitatani F and Furutaka K 2014 *Anal. Chem.* **86** 12030
[2] Festa G, Arcidiacono L, Pappalardo A, Minniti T, Cazzaniga C, Scherillo A, Andreani A and Senesi R 2016 *JINST* **11** C03060
[3] Tian K V, Festa G, Szentmiklósi L, Maróti B, Arcidiacono L, Laganà G, Andreani C, Licoccia S, Senesi R and Cozza P 2017 *J. Anal. At. Spectrom.* **32** 1420
[4] Knoll G F 2000 *Radiation Detection and Measurement* 3rd ed (John Wiley & Sons, Inc.)
[5] Molnár G L, Révay Z and Belgya T 2002 *Nucl. Instrum. Methods Phys. Res. A* **489** 140
[6] *IEEE Std 325-1996 - IEEE Standard Test Procedures for Germanium Gamma-Ray Detectors* (New York, U.S.A.: The Institute of Electrical and Electronics Engineers, Inc.)
[7] Molnár G L (ed) 2004 *Handbook of Prompt Gamma Activation Analysis with Neutron Beams* (Kluwer Academic Publishers)
[8] Fazekas B, Révay Z, Östör J, Molnár G L and Simonits A 1999 *Nucl. Instrum. Methods Phys. Res. A* **422** 469
[9] (Last accessed on February 2018) `http://www.lnhb.fr/nuclear-data/nuclear-data-table/`
[10] (Last accessed on February 2018) `http://www.isis.stfc.ac.uk`
[11] *Hypermet-PC, Version 5.0 - User's Manual* (Budapest, Hungary: Institute of Isotopes)
[12] Zahn G S, Genezini F A and Moralles M *2009 International Nuclear Atlantic Conference - INAC 2009*
[13] Debertin K and Helmer R G 1988 *Gamma- and X-Ray Spectrometry with Semiconductor Detectors* (Amsterdam: North Holland)
[14] Kisab Z, Fazekas B, Östör J, Révay Z, Belgya T, Molnár G L and Koltay L 1998 *Nucl. Instrum. Methods Phys. Res. A* **418**(2) 374
[15] Gadjokov V and Jordanova J 1984 *Comput. Phys. Commun.* **31** 53
[16] *ROOT - An Object-Oriented Data Analysis Framework* (Geneva, Switzerland: CERN)
[17] Festa G, Andreani C, Arcidiacono L, Burca G, Kockelmann W, Minniti T and Senesi R 2017 *JINST* **12** P08005
[18] Andreani C *et al.* 2017 *J. Anal. At. Spectrom.* **32** 1342
[19] Wang T K, Mar W Y, Ying T H, Liao C H and Tseng C L 1995 *Appl. Radiat. Isot.* **46**(9) 933
[20] *Profile HPGe Photon Detector - Product Configuration Guide* (Ortec®)